

DOI: 10.1002/cphc.200((will be filled in by the editorial staff))

# The route to functional graphene oxide

Kinga Haubner<sup>[a]</sup>, Jan Morawski<sup>[b]</sup>, Phillip Olk<sup>[b]</sup>, Lukas M. Eng<sup>[b]</sup>, Christoph Ziegler<sup>[c]</sup>, Barbara Adolphi<sup>[d]</sup> and Evelin Jaehne<sup>\*[a]</sup>

We report on an easy-to-use, successful, and reproducible route to synthesize functionalized graphite oxide (GO) and its conversion into graphene-like materials through chemical or thermal reduction of GO. GO containing hydroxyl, epoxy, carbonyl and carboxyl groups loses mainly hydroxy and epoxy groups during reduction whereas carboxyl species remained untouched. The interaction of functionalized graphene with fluorescent methylene blue (MB) was investigated and compared to graphite, to fully oxidized GO, as well as to thermally and chemically reduced GO. Optical absorption and emission spectra of the composites indicate a clear preference for MB interaction to the GO derivatives containing a high number of functional groups (GO and chemically reduced GO) whereas graphite and thermally reduced

GO only incorporate a few MB molecules. These findings are in consistence with TGA, XPS, and Raman data recorded at every stage of preparation. The optical data also indicate a MB concentration dependent aggregate formation on top of the GO surface, which leads to stable MB dimer and trimer formation on the surfaces. These MB dimers are responsible for fluorescence quenching, which can be controlled by varying the pH value.

## 1. Introduction

Graphite oxide (GO) constitutes of a layered and water-soluble nanomaterial, which is obtained by extensive, chemical oxidation of graphite. [1,2,3] Oxidation creates oxygen containing functional groups at the graphene surface such as hydroxyl, epoxide, carbonyl and carboxyl resulting in polar surface properties. Therefore, GO behaves strongly hydrophilic, and is easily exfoliated in water forming stable colloidal dispersions. [4,5,6] The complete exfoliation into sheets of atomic thickness can also be achieved either by thermal or mechanical treatments. [7,8,9] According to a recently proposed model, GO sheets are composed of planar, graphene-like aromatic domains of a random size interconnected by a network of cyclohexane-like units in chair configuration, which are decorated by the oxygen groups. [10] As synthesized, graphite oxide typically possesses a carbon-to-oxygen ratio of about 2, and the material is non-conducting. Each fundamental layer of GO consists of a dense two-dimensional carbonaceous skeleton [11,12,13] containing a larger number of sp<sup>3</sup> hybridized carbon atoms and a smaller number of sp<sup>2</sup> carbons. [14] GO can be reduced either by heating [7,9] or by reducing agents [15-19], and changes into a graphite-like structure with turbostratic tendency containing few oxygen groups.

The surface chemistry of GO is basically determined by the acidic and basic character of its surface. [20,21,22] The acidic behavior is associated with oxygen complexes or functionalities such as carboxyls, lactones, and phenols. [10] Functionalities like pyrones, chromenes, ethers, and carbonyls are responsible for basic properties of the carbon surfaces. [23] These reactive groups were used to functionalize the graphite oxide surface with, e.g., amino [22], amido [23], p-nitrophenyl [24], isocyanato groups [6], or PEG [25]. Such functionalization improves, for instance, the dispersing of these materials in organic solvents [21] as well

as its miscibility in polymer matrices. [26] Colloidal graphene oxide can be considered as a material with a negative surface charge due to its acidic groups [27,28], and it can be used for constructing multilayer thin films based on electrostatic interactions. [29, 30, 31]

Methylene blue (MB), one of the most commonly used cationic dyes, exhibits two major absorption bands at 293 ( $\pi-\pi^*$ ) and 664 (n- $\pi^*$ ) nm in dilute aqueous solutions, [32] and is known for its pronounced metachromatic behavior and aggregation in various solutions. [33,34]

The aggregation of MB has a significant effect on its optical properties (see Scheme1). The face-to-face (sandwich-type) H-aggregates of this cationic dye shows a blue shift of the spectral band of the  $\pi-\pi^*$  transition, while the head-to-tail (J-type) arrangement reveals a red shift. [35] The H-type aggregates are typically observed in aqueous solutions. While the ~664nm band is assigned to an isolated molecule (monomer), a shift to 605nm accompanied by a second maximum at 697nm is observed when

[a] Dr. Evelin Jähne, Dr. K. Haubner,\* Technische Universität Dresden, Professur für Makromolekulare Chemie, Zellescher Weg 19, 01069 Dresden (Germany)

Fax: (+)49 351 463-37122

E-Mail: evelyn.jaehne@chemie.tu-dresden.de

[b] J. Morawski, Dr. P. Olk, Prof. L. M. Eng, Institut für Angewandte Photophysik, Technische Universität Dresden, George-Bähr-Straße 1, 01069 Dresden (Germany)

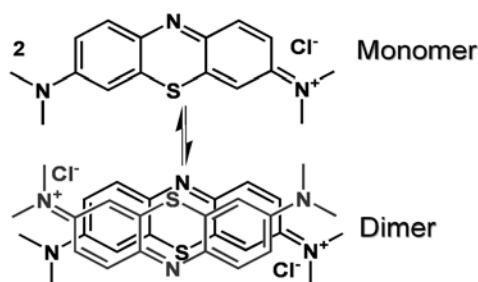
[c] C. Ziegler, Technische Universität Dresden, Professur für Physikalische Chemie, Bergstr. 66b, 01069 Dresden, Germany

[d] Dr. B. Adolphi, Technische Universität Dresden, Institut für Halbleiter- und Systemtechnik, Nöthnitzer Straße 64, 01187 Dresden (Germany)

[+]  
Current address:

Leibnitz-Institut für Festkörper- und Werkstofftechnik Dresden, Institut für Festkörperforschung, Helmholtzstraße 20, 01069 Dresden (Germany)

the dimer forms, and an additional blue shift to 575nm appears upon trimer formation. [36]



**Scheme 1.** Dimerization of Methylene Blue

MB molecular aggregation is strongly dependent on the dye concentration, the dielectric constant of the solvent, the addition of salt, etc. It is known that MB dimerization or aggregation occurs not only in aqueous solution [36] but also on a surface. [37,38]

Boehm already mentioned the interaction of graphite oxide with methylene blue in 1962 using this reaction to determine the surface area of GO. [39] Several authors also described the adsorption of dyes on differently treated carbons. Tryba et al. [40] employed exfoliated and oxidized graphite samples as sorbents for oil and used the adsorption of methylene blue on these substrates as model reaction. Peireira [41] used differently treated carbons for the adsorption experiments showing the existence of two parallel adsorption mechanisms involving electrostatic and dispersive interactions. Yan et al. [42] described MB adsorption on SWNTs driven by charge-transfer and hydrophobic interactions.

Also, the adsorption of MB on different clays has been widely investigated. [43,44] Clay with its layered structure allows a wide range of MB aggregation, which contains intercalation [45], cation exchange [46], as well as fluorescence labeling. [47]

Graphite oxide exhibits a similar layered structure and anionic surface charges as clays. Hence, MB-GO composites should exhibit similar properties compared to the appropriate clay composites. Firstly, we investigate the thermal and optical properties of the GO derivatives with TGA, IR, UV-Vis, XPS and Raman spectroscopy, and secondly, the adsorption behavior of methylene blue on graphite oxide derivatives was additionally examined by fluorescence spectroscopy. Therefore, we use fully oxidized graphite oxide (GO), their chemically and thermally reduced derivatives (GO-C, GO-T), and pristine graphite (PG) for comparison.

## 2. Results and Discussion

### 2.1. Synthesis comment

Graphite oxide was synthesized via a multi-step chemical oxidation reaction after a modified Hummers method. [3] Therefore, commercial graphite was firstly intercalated by H<sub>2</sub>SO<sub>4</sub> treatment, and then oxidized three times with KMnO<sub>4</sub> to achieve a fully oxidized GO. The slurry was repeatedly washed with water, until the pH of the filtrate was neutral, and then the colloidal solution was dialyzed for at least 60 days to remove salt

impurities. The GO powder was dried under vacuum finally resulting in a light brown powder. GO-T, thermally reduced GO, was synthesized by a thermal treatment at 200°C for several hours, whereas GO-C, chemically reduced GO, was obtained via chemical reduction with hydrazine. [8]

### 2.2. Thermal and optical characterization of GO samples

Thermal Gravimetric Analysis (TGA) is a simple analytical technique that measures the weight loss of a material as a function of temperature. As the samples are heated, they lose weight from a simple process such as drying, or from chemical reactions or decompositions that liberate gases.

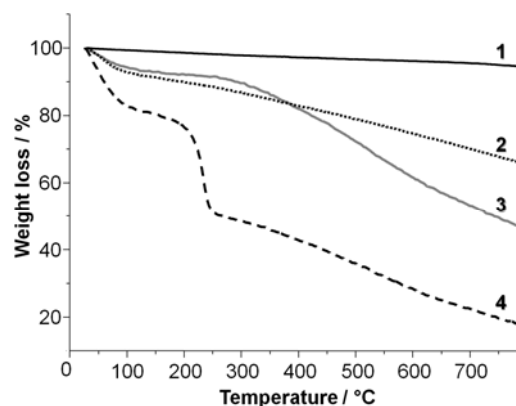


**Figure 1.** TGA of pristine graphite, PG (curve 1), chemical reduced graphite oxide, GO-C (curve 2), thermal reduced graphite oxide, GO-T (curve 3), and graphite oxide, GO (curve 4).

Here, the TGA curves of the GO, pristine graphite PG, and the two reduced GO samples, GO-C and GO-T, are shown in Figure 1. It can be clearly seen that the samples differ in their thermal behaviour. Pristine graphite displays a simple linear dependence, without any steps, indicating a uniform weight loss of physisorbed impurities. In contrast, the TGA curve of GO showed three distinct steps: the weight loss up to 150°C is due to the evaporation of water (~19%), the second one from 150 to 310°C (~30%) is caused by the decomposition of labile oxygen groups (carboxylic, anhydride, or lactone groups), and the third step above 300°C (~30%) is attributed to the removal of more stable oxygen functionalities (such as phenol, carbonyl, quinone) [10].

The thermal and chemical reduced GOs showed much smaller amounts of adsorbed water (~8%) and a higher thermal stability as compared to GO. When comparing the two reduced GOs, the chemical treated GO is more stable than the thermal reduced one.

Table 1. Atomic concentration of graphite, GO, GO-C, GO-T [%]				
Sample	Elements			
	C1s	N1s	O1s	O/C ratio
PG	98.6		1.4	0.014
GO	62.2	0.4	36.4	0.582
GO-T	73.7	0.9	23.0	0.312
GO-C	74.8	7.5	15.7	0.209

XPS measurements of the different samples were performed to gain information about their composition, the degree of oxidation and the kind of oxygen species present. Table 1 shows the atomic concentration of all samples. The initial oxygen concentration of graphite was only a small proportion of 1.4%, but after oxidation it increased to 36.4% along with the reduction of carbon content. After thermal reduction the oxygen content decreased to 23.0%, whereas after chemical reduction the oxygen content became 15.7% accompanied with an increase of nitrogen due to the incorporation of hydrazine.

The detailed C1s spectrum of GO (Figure 2) revealed five peaks, which were assigned to the following groups: C1s (1) to  $sp^2$ -carbon at 284.4 eV, C1s (2) to  $sp^3$ -carbon at 285.2 eV, C1s (3) to C-OH at 286.4 eV, C1s (4) to C=O at 287.7 eV and C1s (5) to COOH at 289.1 eV.

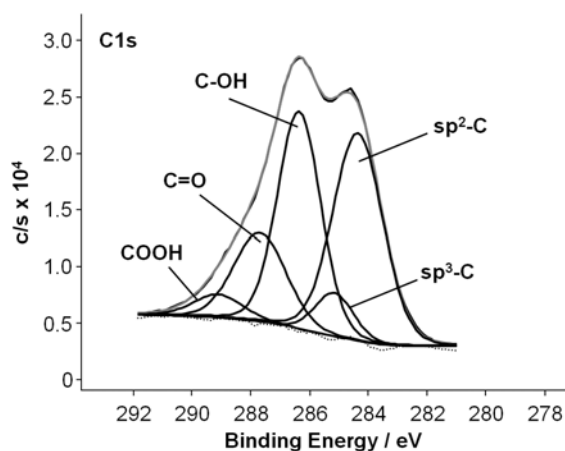


Figure 2. High resolution XPS C1s single spectrum of GO.

The presence of  $sp^3$ -carbon and the high content of oxidized species are the proof for the change of graphite structure due to oxidation. The results are consistent with the high resolution O1s spectrum of GO (Figure 3). The content of double bond oxygen (C=O, COOH) is about 30%, and the single bond (C-OH, epoxy) was 54%. Additionally, 16% water was found.

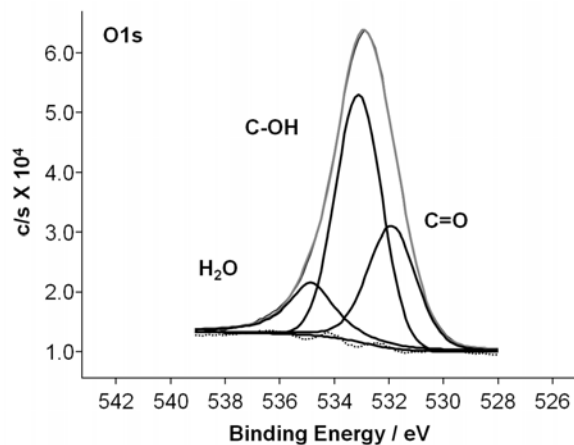


Figure 3. High resolution XPS O1s single spectrum of GO.

After reduction either thermally or chemically, the ratios of the different peaks changed. As an example, the high resolution C1s and O1s spectra of thermally reduced GO are represented in Figures 4 and 5. The  $sp^2$ -C peak increases as well the C-OH and C=O peaks decrease, whereas the COOH peak does not change. Additionally, the  $\pi$ - $\pi^*$  shake-up peak is visible in both reduced derivatives, which is a proof for the increase of aromaticity within these layers. The decrease of hydroxyl and epoxy groups in relation to the carbonyl and carboxyl ones is also visible in the appropriate O1s spectra.

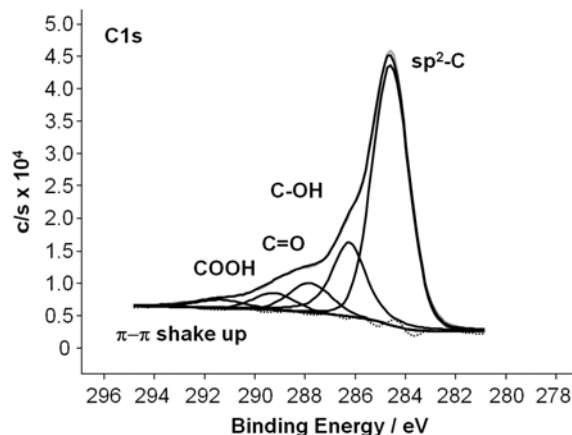


Figure 4. High resolution XPS C1s single spectrum of GO-T.

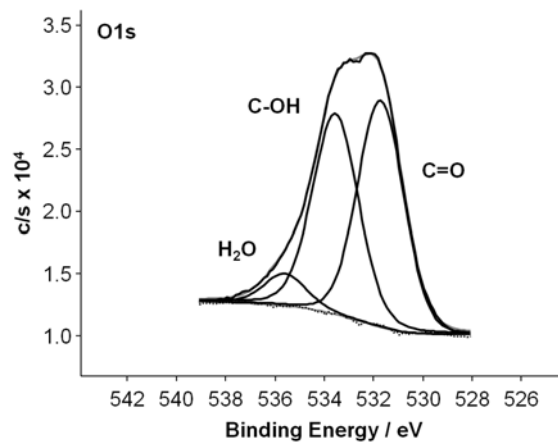


Figure 5. High resolution XPS O1s single spectrum of GO-T

Sample	C1s					
	$sp^2$ -C	$sp^3$ -C	-C-OH	-C=O	-COOH	$\pi$ - $\pi$
Graphite	65.5	21.8	-	5.2	3.4	4.0
GO	38.0	6.2	34.4	17.0	4.5	-
GO-T	62.5	-	20.3	8.5	5.0	3.6
GO-C	54.4	-	28.2	8.2	4.7	4.5

Table 2 summarizes all results. The high content of oxygen groups in GO gives proof for a highly oxidized sample. The reduction resulted in two similar derivatives, where on the one hand especially the hydroxyl content decreased and the C=O

groups were bisected, while on the other hand, the number of carboxyl groups remained unchanged.

Raman spectroscopy was used as powerful, nondestructive tool in order to characterize carbon materials, particularly for distinguishing their ordered and disordered crystal structures. The typical features for carbon in Raman spectra are the G line around  $1582\text{cm}^{-1}$  and the D line around  $1350\text{cm}^{-1}$ . The G line is usually assigned to the  $E_{2g}$  phonon of C  $sp^2$  atoms, while the D line is a breathing mode of  $k$ -point phonons of  $A_{1g}$  symmetry. Extensive studies have determined that the positions, intensities and widths of these bands are dependent on the ordering of the  $sp^2$  sites in varying compositions of amorphous and crystalline carbon compounds. [48,49,50] Figure 6 shows Raman spectra of pristine graphite and the three GO derivatives. The Raman spectrum of the pristine natural graphite displays a strong G peak at  $1580\text{cm}^{-1}$ , a weak D line at  $1350\text{cm}^{-1}$ , the overtone of the D line, the 2D line, located at  $2723\text{cm}^{-1}$  (not shown) and a very weak D' line at  $1619\text{cm}^{-1}$ . In the Raman spectrum of GO, the G band is broadened and shifted slightly to  $1583\text{cm}^{-1}$ , whereas the intensity of the D band at  $1350\text{cm}^{-1}$  increases substantially and the 2D line disappeared. These phenomena could be attributed to the significant decrease of the size of the in-plane  $sp^2$  domains due to oxidation and ultrasonic exfoliation. [8] We found that all three GO samples gave a similar Raman spectrum in terms of the shapes and positions of Raman peaks.

The significant increase in the D/G area ratio of all GO derivatives compared to pristine graphite also indicates a decrease in the size of the in-plane  $sp^2$  domains. The results imply that the graphitic structure of the GO derivatives could not be restored after both the chemical or thermal reduction.

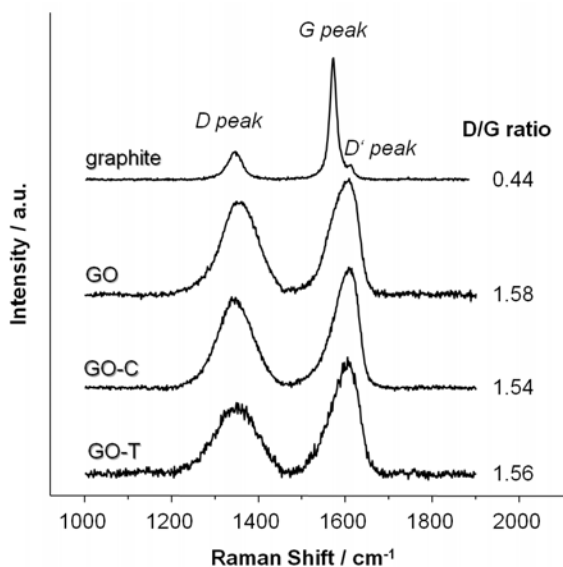


Figure 6. Comparison of Raman spectra of all graphitic derivatives.

### 2.3. Investigation of GO-MB composites

MB is a cationic dye, which is adsorbed mainly by electrostatic forces on a negative surface. Therefore, MB immediately forms stable composites, when it is adsorbed on highly reactive GO.

We investigated this composite with IR spectroscopy to give proof, whether this reaction was successful or not, visible in

Figure 7 displaying the FTIR spectra of GO, MB, and the GO-MB composite. The broad band at  $3400\text{cm}^{-1}$  of GO belongs to the  $\nu(\text{OH})$  vibration and the band at  $1626\text{cm}^{-1}$  is significant to the deformation vibration of O-H groups.  $\nu(\text{C}=\text{O})$  at  $1735\text{cm}^{-1}$  is assigned to the carbonyl and carboxyl moieties, and the vibration at  $1065\text{cm}^{-1}$  is assigned to  $\nu(\text{C}-\text{O})$  band of the epoxy group. After adsorption the  $\nu(\text{O}-\text{H})$  at  $3400\text{cm}^{-1}$  remained unchanged, whereas the  $\nu(\text{C}=\text{O})$  peak decreased and shifted to higher wavenumbers. This also indicates that MB was loaded onto GO, and the shift of characteristic peaks may be due to the hydrogen bonding between these two components.

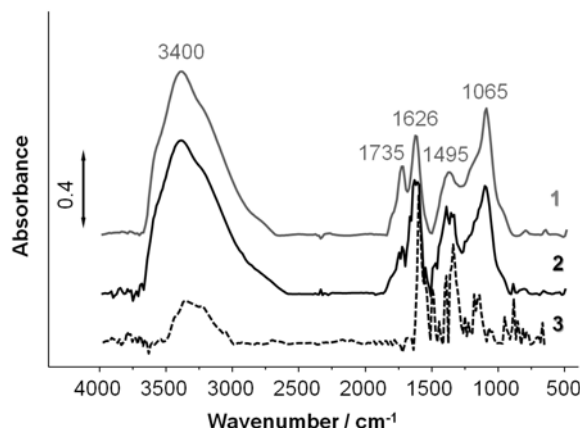


Figure 7. FT-IR spectra of GO (curve 1), MB adsorbed on GO (curve 2) and solid MB (curve 3).

As cationic dye methylene blue is very well detectable by UV-Vis spectroscopy. MB in aqueous solution has a blue color with a strong absorbance at  $664\text{nm}$  that is characteristic for the MB monomer in solution. The shoulder at  $613\text{nm}$  is assigned to MB dimerization in solution. Figure 8 shows the changes of MB intensities after adsorption on the GO derivatives.

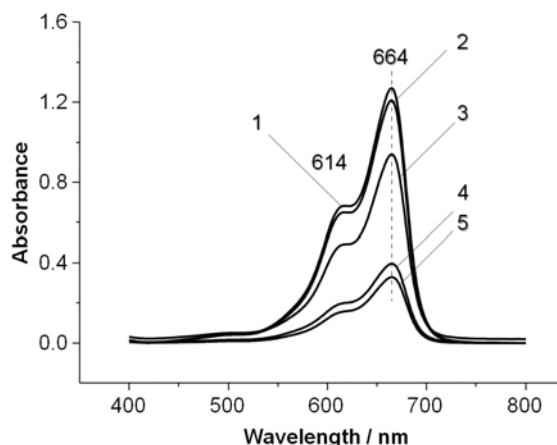


Figure 8. UV-Vis spectra of aqueous solution of MB ( $10^{-5}\text{M}$ ) (curve 1), MB adsorbed on PG (curve 2), MB adsorbed on GO-T (curve 3), MB adsorbed on GO-C (curve 4) and MB adsorbed on GO (curve 5).

The intensity of MB decreases in the range of adsorbents from graphite to graphite oxide. Due to the negatively charged surface of graphite oxide (C-OH, COOH), this material was the most effective adsorbent for MB followed by chemically and

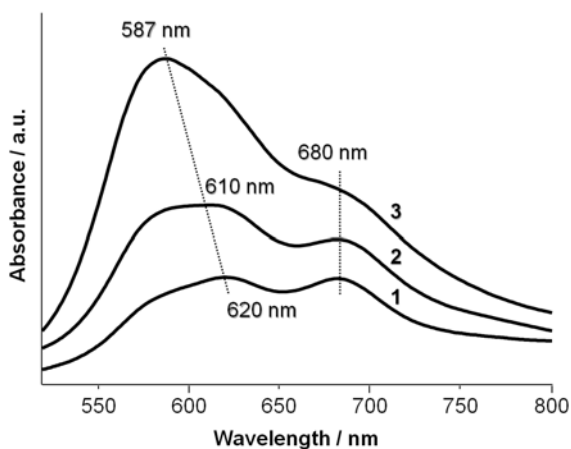
thermally reduced GOs. In comparison, graphite adsorbed only a small amount of MB.

The loading was calculated after equation 1:

$$Q = (M_{MB} - M_{MB}^*)/M_{GO} \quad (1)$$

where Q is the loading of MB on the substrates in mg/mg,  $M_{MB}$  is the initial MB mass in mg and  $M_{MB}^*$  is the residue mass in the adsorption solution in mg. GO adsorbed 0.0241mg/mg, GO-C 0.0227mg/mg, GO-T 0.0099mg/mg and graphite 0.0035mg/mg.

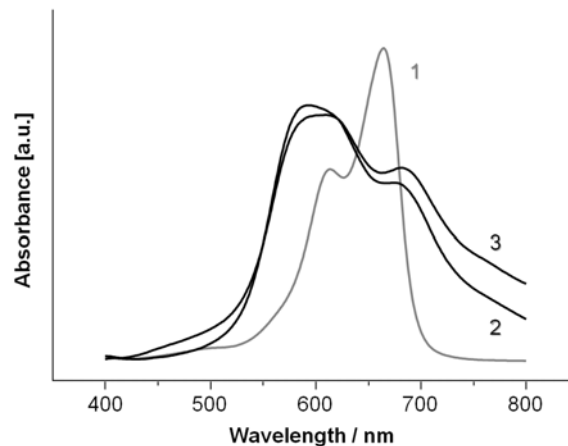
Because GO adsorbs the highest amount of MB, this combination was used in model reactions to investigate the influence of MB concentration and adsorption time on forming MB-GO composites.



**Figure 9.** Comparison of UV-Vis spectra of MB-GO dispersions from different MB concentrations:  $10^{-5}$  M (curve 1),  $2.5 \times 10^{-5}$  M (curve 2),  $5 \times 10^{-5}$  M (curve 3) ( $c_{GO} = 0.1$  g/l, adsorption time 24h).

In Figure 9 the UV-Vis spectra are visualized, which were recorded from MB-GO composites derived from different MB concentrations: as bigger the MB concentration as higher the dye absorption in UV-Vis spectra. Depending on concentration also the shape of the curves changed, and therefore, the type of aggregation. At high concentrations (curve 3) the peak maximum is located at 587nm indicating a trimer formation of MB on the substrate. With decreasing concentration the peak maxima of the curves shifted to higher wavelength (bathochromic shift) caused by a decrease of MB aggregation on the GO surface. The second maximum at 680nm assigned to adsorbed monomer (in curve 3 visible as shoulder) increased with decreasing concentration, but did not shift.

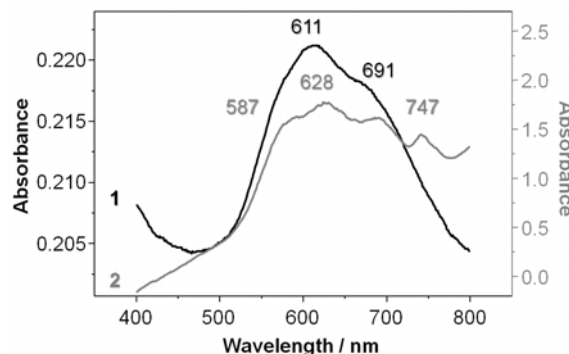
Figure 10 shows the UV-Vis spectra of MB-GO adsorption solutions at different adsorption times compared to the aqueous MB solution. Immediately after mixing both solutions, the UV maxima (red curve) split and shifted to lower as well as to higher wavelength. After 24h the change in UV-Vis spectrum was marginal indicating a small rearrangement of the MB aggregates on GO.



**Figure 10.** UV-Vis spectra of  $2.5 \times 10^{-5}$  M MB solution (curve 1), MB-GO nanostructure, immediately after mixing in water (curve 2, with 4x amplification), and after 24h adsorption time (curve 3, with 4x amplification).

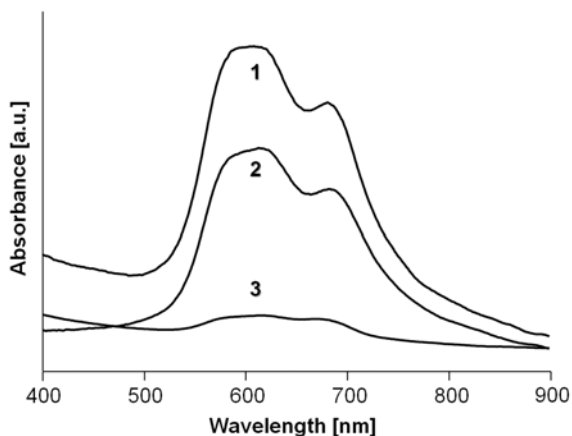
Therefore, one can conclude that MB aggregates on GO in different shapes depending mainly on MB concentration, whereas the adsorption time does not play an important role.

Figure 11 depicts the UV-Vis spectra of MB-GO composites adsorbed from  $5 \times 10^{-5}$  M solution with 24h adsorption time: on the one hand as dispersion in water (curve 1) and on the other hand, as dry film on quartz (curve 2). Compared to the MB spectrum in solution (see Figure 9) both samples show important differences in the positions of peak maxima. The MB-GO dispersion exhibits two maxima at 611nm and 691nm assigned to adsorbed MB dimer and monomer, respectively. The spectrum of the film presents one additional absorption maximum at 747nm compared to the dispersion. This new band is due to the aggregation of the dye (dimerization) on the GO surface. The shoulder at 587nm in suspension and in film is attributed to trimer and/or higher aggregates of MB. The shoulders at 628nm for the film and 691 nm for suspension indicate a bathochromic shift to lower energies which assigned adsorption of MB monomer onto the GO surface. The band at 747nm can be explained due to the formation of L-dimers. [51]



**Figure 11.** UV-Vis absorption spectra of MB-GO composites: MB-GO dispersed in water (curve 1), MB-GO solid film on quartz (curve 2) ( $c_{MB} = 5 \times 10^{-5}$  M,  $c_{GO} = 0.1$  g/l, adsorption time 24h).

Table 3. Characteristic bands of adsorbed MB			
MB-GO dispersion		MB-GO film on quartz	
$\lambda_{max}$ [nm]	assignment	$\lambda_{max}$ [nm]	assignment
587	MB <sub>3</sub>	587 sh	MB <sub>3</sub> adsorbed
611	MB <sub>2</sub>	628	MB <sub>2</sub> adsorbed
691 sh	MB	~700	MB
		747	MB <sub>2</sub> L-form [51]



**Figure 12.** UV-Vis absorption spectra of MB-GO dispersions (curve 1), MB-GO after treatment with ultrasound (curve 2), MB solution after centrifugation (curve 3) ( $C_{MB} = 5 \times 10^{-5} M$ ,  $C_{GO} = 0.1 g/l$ ).

Stability of the MB-GO composite was tested by ultrasonic treatment (Figure 12). One can clearly see that after the usage of ultrasound the intensity of the UV-Vis spectrum decreased. But the shape of the curve did not change indicating that the kind of MB aggregation on GO surface did not alter, too.

All these results indicate that different MB aggregates are present on the GO surface. In contrast to similar investigations on MB-clay composites [43,46] the appropriate structures on GO do not change with adsorption time. It can be concluded that the interaction of MB with the reactive oxygen groups of the GO surface is stronger than that with the surface hydroxyls of clays.

Raman spectra of graphite, GO, thermally and chemical reduced GO with MB are presented in Figures 13-16.

As Figures 13 and 14 show, the aggregation of MB on graphite and GO, respectively, leads to a slightly reduced Raman signal, if compared to the pure carbon substances. But while the Raman signal of pure graphite is just damped containing few parts of MB, the Raman spectrum of GO-MB composite is clearly reproducing the Raman spectrum of pure MB accompanied with a disappearance of G and D bands originated from GO. The results are caused by the different amounts of aggregated MB on these substrates, and they are in full agreement with the findings from UV-Vis measurements.

Comparing the Raman spectra of the GO-C and GO-T MB composites (Figures 15, 16) one can see that on one hand the different adsorbed MB amount on both substrates and on the other hand the different surface composition influenced the composite spectra. The part of  $sp^2$  carbon, which is high for

graphite and GO-T seems to be unable to adsorb MB. In the case of GO-C and GO we can find a partial and full adsorption of MB, respectively.

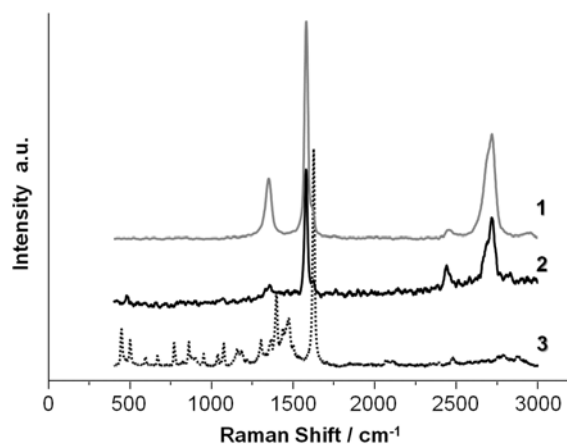


**Figure 13.** Raman spectra of graphite (curve 1), MB adsorbed on graphite (curve 2), and solid MB (curve 3) (excited at 532nm).

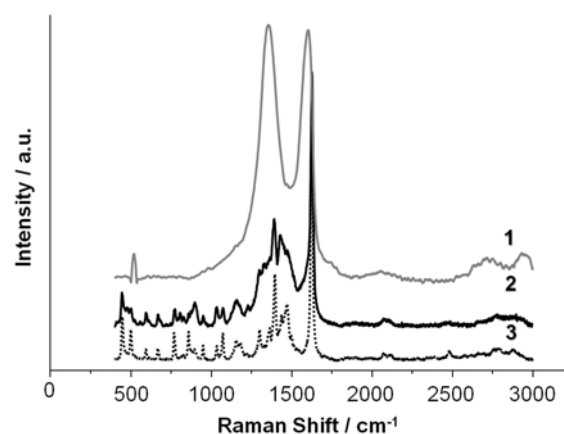


**Figure 14.** Raman spectra of GO (1), MB adsorbed on GO (2) and solid MB (3). (excited at 532nm)

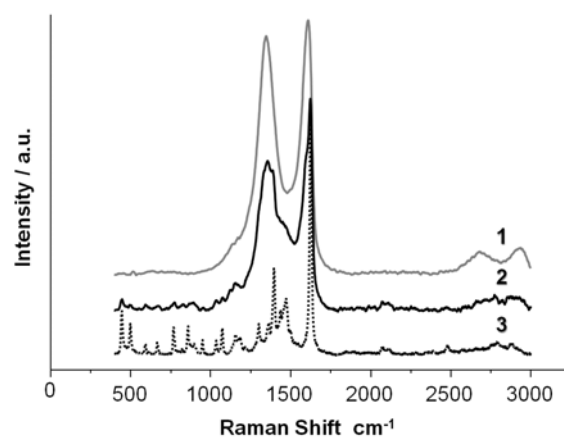


**Figure 15.** Raman spectra of GO-C (1), MB adsorbed on GO-C (2) and solid MB (3). (excited at 532nm)

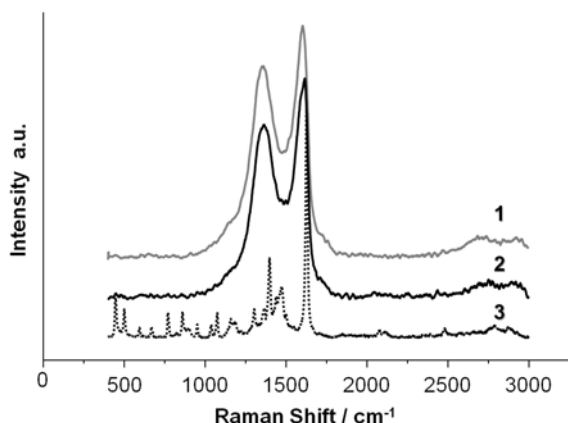


**Figure 16.** Raman spectra, excited at 532 nm of GO-T (1), MB adsorbed on GO-T (2) and solid MB (3).

Thiazine dyes including methylene blue (MB) are well-known groups of dyes, which are strongly fluorescent.

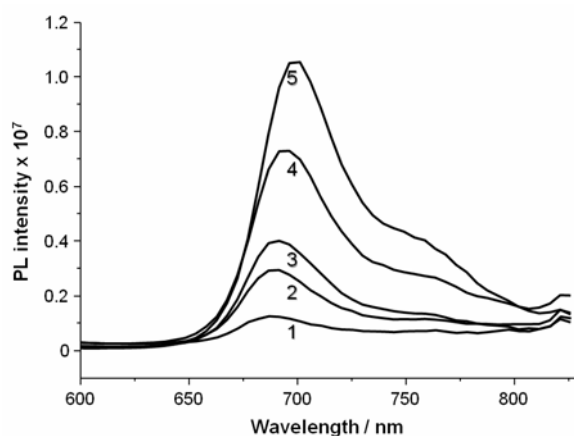


**Figure 17.** Emission spectra of aqueous solution of MB at different concentrations:  $2.5 \times 10^{-6}$  (1),  $5 \times 10^{-6}$  (2),  $10^{-5}$  (3),  $2.5 \times 10^{-5}$  (4),  $5 \times 10^{-5}$  (5), (excitation wavelength 620 nm).

It is well known phenomenon that the fluorescence of many dyes is quenched in a concentrated solution or after adsorption of the dye on solid substrates. This is understood to be due to association of the dye, as explained in 2.3. It has been established that in ethanol solution MB is present predominantly as monomers, while it forms face-to-face dimers in aqueous solution, which exist in dynamic equilibrium with monomers.

After adsorption of MB on GO the fluorescence signal of the dye decreased or disappeared. This is explained by dimer formation on the GO surface. pH dependent fluorescence measurements (Figure 18) revealed that at conditions from acidic up to light basic (pH from 3 to 10) the fluorescence is quenched, whereas in strong basic environment (pH from 11 to 13) fluorescence rapidly increased. At this pH range the acidic groups are transformed into their salts resulting in weakening electrostatic as well as hydrogen bond interactions of MB with the substrate.

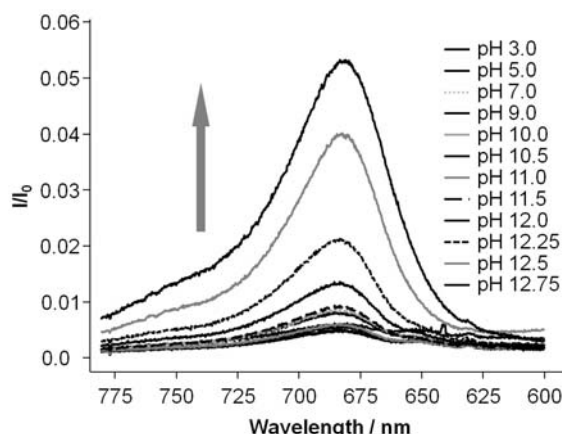


**Figure 18.** Emission spectra of aqueous solution of MB-GO composite at different pH values ( $C_{MB} = 5 \times 10^{-5}$  M,  $C_{GO} = 0.1$  g/l, adsorption time 24h, excitation wavelength 532 nm, 0.5 mW, 60x1s).

### 3. Conclusion

We report here on an easy, successful, and reproducible route to synthesize functionalized graphite oxide (GO) containing hydroxyl, epoxy, carbonyl and carboxyl groups. This material is hydrophilic and forms stable suspensions in water and other solvents. Thermal investigations by TGA measurements revealed the high content of incorporated water (~16%). GO was converted into graphene-like materials through chemical and thermal reduction processes. XPS and Raman spectroscopy gave proof of partly reduction of single bound oxygen whereas the carboxyl functionalities remained untouched. Although the oxygen content decreased during reduction the size of the in-plane  $sp^2$  domains was also decreased due to oxidation and ultrasonic exfoliation.

Interaction of the GO derivatives with fluorescent methylene blue (MB) was investigated and the results show that depending on the number and kind of reactive oxygen groups different amounts of MB were adsorbed. The dye molecules formed stable aggregates on the substrates, which were investigated by UV-Vis, fluorescence and Raman spectroscopy. Optical absorption and emission spectra of the composites indicate a clear preference for MB interaction to the GO derivatives containing a high number of functional groups (GO and chemically reduced GO) whereas graphite and thermally reduced GO only incorporate a few MB molecules. The formed dimer and trimer MB aggregates on GO quench fluorescence of MB. By variation of pH value the strong electrostatic interaction can be weakened at high pH leading to increase of fluorescence intensity.

Further studies are now under investigation regarding chemical derivatization of GO with the aim to tune GO surface properties. The results will be published soon.

### Experimental Section

GO was synthesized by a modified Hummers method [3]. Briefly, 5g graphite (synthetic graphite powder, <math>20\mu\text{m}</math>, Sigma-Aldrich) were immersed in  $\text{H}_2\text{SO}_4$  conc. (160 mL) and  $\text{NaNO}_3$  (5g, 0.059mol) under stirring for 1h in an ice bath.  $\text{KMnO}_4$  (23g, 0.145mol) was slowly

added, and the mixture was stirred under cooling for 2h, and further at room temperature for five days. The reaction suspension was carefully diluted with 500mL aqueous H<sub>2</sub>SO<sub>4</sub> (5wt%) [Caution! Temperature increases rapidly!], and further stirred for 2h. 15mL H<sub>2</sub>O<sub>2</sub> (30wt% aqueous solution) was added, and the mixture was kept under stirring for 2h. The reaction mixture was carefully washed with water, centrifuged (3 times), and dialyzed for at least 60 days to remove salt impurities. Finally, the material was dried in vacuum oven to get a loose, light brown powder. Chemically reduced GO was obtained by reduction with hydrazine hydrate [8]. For thermal reduction, GO powder was heated from room temperature to 200°C in a vacuum furnace for 5h and then ramped down to room temperature within 5h.

TGA measurements were carried out using a TA instruments DSC 2920. The measurements were performed at a scan rate of 10K/min under nitrogen atmosphere.

The XPS experiments were carried out on a Physical Electronics PHI 5700 ESCA System with Auger-Spectroscopy using a non-monochromatic Mg K $\alpha$  X-ray source operating at 400W power consumption. Spectra were acquired at a base pressure of 10<sup>-9</sup> mbar. The instrument was run in a minimum-area mode using an aperture of 0.8mm<sup>2</sup>. The obtained peak areas were normalized with sensitive factors. Electron binding energies were calibrated against the alkyl C1s emission peak at 285eV. Detector angle  $\theta$ , defined as the angle between the electron kinetic energy analyzer and the sample surface, was fixed at 45° for all the XPS experiments.

Infrared (IR) spectra were recorded with Nicolet 6700 FT-IR Spectrometer, using KBr pellets.

UV-Vis measurements: UV-Vis spectra were taken on a Perkin-Elmer Lambda 35 in 1cm quartz cuvettes. The concentration of aqueous MB stock solution was 5x10<sup>-4</sup>M. The used concentrations ranged from 10<sup>-5</sup>M to 5x10<sup>-4</sup>M. Adsorption were carried out at room temperature (25°C) using 100mL of MB solution and 10mg of adsorbent (pristine graphite, chemically reduced GO and thermally reduced GO), which were shaken for 12h. After adsorption the solutions were centrifuged and measured by UV-Vis spectroscopy. The precipitated powders were washed three times with distilled water and dried in vacuum oven at 40°C. 2mg of each composite were dissolved in 5mL water containing 0.2% Tween80<sup>®</sup> as surfactant. The suspensions were shaken for 5min and immediately measured. The content of adsorbed MB was estimated by measuring absorbance at maximum wavelength and calculated from calibration curves.

Fluorescence measurements were performed on Max-2 spectrofluorimeter (Instruments SA, Edison, NJ, USA). All spectra were recorded at room temperature, 25±1°C.

Raman spectra were obtained on a confocal Raman spectrometer (Renishaw RM 2000, England). A 532nm argon ion laser was used as the excitation source. A 50x objective was used, giving a spot size of 3 $\mu$ m in diameter. The Raman spectra were taken every 120s for data accumulation. The laser power on the sample was at 5 $\mu$ W. Spectra were calibrated using the 520cm<sup>-1</sup> band of silicon.

## Acknowledgements

We would like to thank A. Nikol and R. Luther for performing IR and UV-Vis measurements. Financial support was provided by the Deutsche Forschungsgemeinschaft (DFG).

**Keywords:** graphite oxide (GO), reduced GO, methylene blue-graphite oxide composites, optical spectroscopy

- [1] B. C. Brodie, *Ann. Chim. Phys.* **1890**, *59*, 466-472.
- [2] L. Staudenmaier, *Ber. Dtsch. Chem. Ges.* **1898**, *31*, 1481-1487.
- [3] W. S. Hummers, and R. E. Offerman, *J. Am. Chem. Soc.* **1958**, *80*, 1339-1339.
- [4] S. Park, J. An, R. D. Piner, I. Jung, D. Yang, A. Velamakanni, S.-B. T. Nguyen, and R. S. Ruoff, *Chem. Mater.* **2008**, *20*, 6592-6594.
- [5] Y. Si and E. T. Samulski, *Nano Lett.* **2008**, *8*, 1679-1682.
- [6] S. Stankovich, R. D. Piner, S.-B. T. Nguyen, and R. S. Ruoff, *Carbon* **2006**, *44*, 3342-3347.
- [7] H. C. Schniepp, J.-L. Li, M. J. McAllister, H. Sai, M. Herrera-Alonso, D. H. Adamson, R. K. Prud'homme, R. Car, D. A. Saville, and I. A. Aksay, *J. Phys. Chem. B* **2006**, *110*, 8535-8539.
- [8] S. Stankovich, D. A. Dikin, R. D. Piner, K. A. Kohlhaas, A. Kleinhammes, Y. Jia, Y. Wu, S. T. Nguyen, and R. S. Ruoff, *Carbon* **2007**, *45*, 1558-1565.
- [9] M. J. McAllister, J.-L. Li, D. H. Adamson, H. C. Schniepp, A. A. Abdala, J. Liu, M. Herrera-Alonso, D. L. Milius, R. Car, R. K. Prud'homme, and I. A. Aksay, *Chem. Mater.* **2007**, *19*, 4396-4404.
- [10] T. Szabo, O. Berkesi, P. Forgo, K. Josepovits, Y. Sanakis, D. Petridis, and I. Dekany, *Chem. Mater.* **2006**, *18*, 2740-2749.
- [11] A. Lerf, H. He, M. Forster, and J. Klinowski, *Structure J. Phys. Chem. B* **1998**, *102*, 4477-4482.
- [12] D.-Q. Yang, and E. Sacher, *Surf. Sci.* **2002**, *504*, 125-129.
- [13] D. Wan, and K. Komvopoulos, *J. Phys. Chem. C*, **2007**, *111*, 9891-9896.
- [14] R. Muszynski, B. Seger, and P. V. Kamat, *J. Phys. Chem. C* **2008**, *112*, 5263-5266.
- [15] D. Li, M. B. Muller, S. Gilje, R. B. Kaner, G. G. Wallace, G. G. *Nat. Nanotechnol.* **2008**, *3*, 101-105.
- [16] G. Williams, B. Serger, p. V. Kamat, *ACS Nano* **2008**, *2*, 1487-1491.
- [17] Y. Xu, H. Bai, G. Lu, C., and G. Shi, *J. Am. Chem. Soc.* **2008**, *130*, 5856-5857.
- [18] V. C. Tung, M. J. Allen, Y. Yang, R. B. Kaner, *Nat. Nanotechnol.* **2009**, *4*, 25-29.
- [19] H. P. Boehm, *Carbon* **1994**, *32*, 759-769.
- [20] M. V. Lopez-Ramon, F. Stoeckli, C. Moreno-Castilla, and F. Carrasco-Marin, *Carbon* **1999**, *37*, 1215-1221.
- [21] E. Fuente, J. A. Menéndez, D. Suárez, and M. A. Montes-Morán, *Langmuir* **2003**, *19*, 3505-3511.
- [22] A. B. Bourlinos, D. Gournis, D. Petridis, T. Szabó, A. Szeri, and I. Dékány, *Langmuir* **2003**, *19*, 6050-6055.
- [23] S. Niyogi, E. B., M. E. Itkis, J. L. McWilliams, M. A. Hamon, and R. C. Haddon, *J. Am. Chem. Soc.* **2006**, *128*, 7720-7721.
- [24] E. Bekyarova, M. E. Itkis, P. Ramesh, C. Berger, M. Sprinkle, W. A. de Heer, and R. C. Haddon, *J. Am. Chem. Soc.* **2009**, *131*, 1336-1337.
- [25] Z. Liu, J. T. Robinson, X. Sun, and H. Dai, *J. Am. Chem. Soc.* **2008**, *130*, 10876-10877.
- [26] S. Stankovich, D. A. Dikin, G. H. B. Dommett, K. M. Kohlhaas, E. J. Zimney, E. A. Stach, R. D. Piner, S.B. T. Nguyen and R. S. Ruoff, *Nature* **2006**, *442*, 282-286.
- [27] I. Dekany, R. Kruger-Grasser, and A. Weiss, *Coll. Polym. Sci.* **1998**, *276*, 570-576.
- [28] N. A. Kotov, I. Dekany, and J. H. Fendler, *Adv. Mater.* **1996**, *8*, 637-641.
- [29] T. Cassagneau, and J. H. Fendler, *Adv. Mater.* **1998**, *10*, 877-881.
- [30] T. Cassagneau, F. Guerin, and J. H. Fendler, *Langmuir* **2000**, *16*, 7318-7324.
- [31] N.T. Kovtyukhova, P. Ollivier, B. R. Martin, T. E. Mallouk, S. A. Chizhik, E. V. Buzaneva, and A. D. Gorchinskiy, *Chem. Mater.* **1999**, *11*, 771-778.
- [32] C. Parkanyi, C. Boniface, J. J. Aaron, and M. Maafi, *Spectrochim. Acta, Part A* **1993**, *49*, 1715-1725.
- [33] K. Bergmann, and C. T. O'Konski, *J. Phys. Chem.* **1963**, *67*, 2169-2177.
- [34] E. Braswell, *J. Phys. Chem.* **1967**, *72*, 2477-2483.
- [35] K. Kemnitz, N. Tamai, I. Yamazaki, N. Nakashima, and K. Yoshihara, *J. Phys. Chem.* **1986**, *90*, 5094-5101.
- [36] C. H. Giles, D. G. Duff, and A. *Water: A Comprehensive Treatise*; Franks, Ed.; New York, 1973.
- [37] S. M. Ohline, S. Lee, S. Williams, and C. Chang, *Chem. Phys. Lett.* **2001**, *346*, 9-15.
- [38] H. Kobayashi, M. Takahashi, and M. Kotani, *Chem. Phys. Lett.* **2001**, *349*, 376-382.
- [39] H. P. Boehm, A. Clauss, G. O. Fischer, and U. Hofmann, *Z. Anorg. Allg. Chem.* **1962**, *316*, 119-127.

- [40] B. Tryba, A. W. Morawski, R. J. Kaleńczuk, and M. Inagaki, *Spill Sci. Technol. Bull.* **2003**, *8*, 569-571.
- [41] M. F. R. Pereira, S. F. Soares, J. J.M. Órfão, and J. L. Figueiredo, *Carbon* **2003**, *41*, 811-821.
- [42] Y. Yan, M. Zhang, K. Gong, L. Su, Z. Guo, and L. Mao, *Chem. Mater.* **2005**, *17*, 3457-3462.
- [43] F. Gessner, C. C. Schmitt, and M. G. Neumann, *Langmuir* **1994**, *10*, 3749-3753.
- [44] J. Bujdák, A. Czimerová, and N. Iyi, *Thin Solid Films* **2008**, *517*, 793-796.
- [45] M. Hajjaji, and A. Alami, *App. Clay Sci.* **2009**, *44*, 127-132.
- [46] M. G. Neumann, F. Gessner, C. C. Schmitt, and R. Sartori, *J. Coll. Inter. Sci.* **2002**, *255*, 254-259.
- [47] Z. Klika, P. Čápková, P. Horáková, M. Valášková, P. Malý, R. Macháň, and M. Pospíšil, *J. Coll. Inter. Sci.* **2007**, *311*, 14-23.
- [48] C. Vix-Guterl, M. Couzi, J. Dentzer, M. Trinquescoste, and P. Delhaes, *J. Phys. Chem. B* **2004**, *108*, 19361-19367.
- [49] F. Tuinstra, J.L. Koenig, *J. Chem. Phys.* **1970**, *53*, 1126-1130.
- [50] A.C. Ferrari, J. Robertson, *Phys. Rev. B* **2000**, *61*, 14095-14107.
- [51] K. Y. Jacobs, and R. A. Schoonheydt, *J. Coll. Inter. Sci.* **1999**, *220*, 103-111.

---

Received: ((will be filled in by the editorial staff))

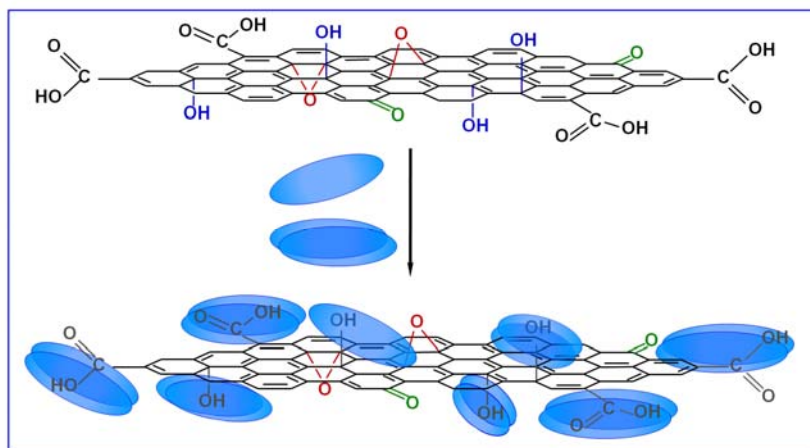
Published online: ((will be filled in by the editorial staff))

---

## Entry for the Table of Contents

### ARTICLES

---



*Kinga Haubner, Jan Morawski, Phillip Olk, Lukas M. Eng, Christoph Ziegler, Barbara Adolphi and Evelin Jaehne\**

**Page 1. – Page 9.**

**The route to functional graphene oxide**

Interaction of methylene blue (MB) with functionalized graphene oxide (GO) leads to the generation of stable MB-GO composites. MB dimers aggregate on the GO surface inducing a change of optical properties of the composite. UV-Vis absorption bands shift to lower wavelength and fluorescence is quenched due to dimer formation. By variation of pH value the strong electrostatic interaction can be weakened at high pH leading to increase of fluorescence intensity.